Visual Features based Boosted Classification of Weeds for Real-Time Selective Herbicide Sprayer Systems

Abstract

Recent years have shown enthusiastic research interest in weed classification for selective herbicide sprayer systems which are helpful in eradicating unwanted plants such as weeds from fields, minimizing the side effects of chemicals on the environment and crops. Two commonly found weeds are monocots (thin leaf) and dicots (broad leaf), requiring separate chemical herbicides for eradication. Researchers have used various computer vision-assisted techniques for eradication for these weeds. However, the changing and un-predictive lighting conditions in fields make the process of weed detection and identification very challenging. Therefore, in this paper, we present an efficient weed classification framework for real-time selective herbicide sprayer systems, exploiting boosted visual features of images, containing weeds. The proposed method effectively represents the image using local shape and texture features which are extracted during the leaf growth stage using an efficient method, preserving the discrimination between various weed species. Such effective representation allows accurate recognition at early growth stages. Furthermore, the various illumination problems prior to feature extraction are minimized using an adaptive segmentation algorithm. AdaBoost with Naïve Bayes as a base classifier discriminates the two weed species. The proposed method achieves an overall accuracy 98.40%, with true positive rate of 0.983 and false positive rate of 0.0121 for the original dataset and achieved 94.72% accuracy with the expanded dataset. The execution time of the proposed method is about 35 millisecond per image, which is less than state-of-the-art methods.

Keywords

Weed Classification, Machine Learning, Computer Vision, Image Segmentation, Selective Herbicide Sprayer Systems, Boosted Classifier for Weed Detection

1. Introduction

Elimination of unnecessary plants such as weeds from fields is one of the tedious jobs for farmers on a regular basis. Weeds in fields result in various issues such as competing for water,

nutrients, light, and space; reducing crop yields; and affecting the surrounding environment [1]. To eradicate these weeds from fields, chemical herbicides [2] can be effectively used. Herbicides must be applied in a way to successfully eliminate weeds, avoiding their unwanted effects on remaining crops and environment [3, 4]. In a recent study, Laursen et al. [4] presented an algorithm to segment and quantify weeds in Maize crops in order to reduce herbicide usage. Their study revealed that the selective application of herbicides reduces its usage by 65%. Weeds may grow in patches or individually, however, applying herbicides equally on all parts of the field is not an efficient way. In this case, the sprayer system should apply spray selectively on the concerned regions of the fields only [5]. Computer vision-directed approaches are helpful in this regard to develop smart sprayer systems which can selectively spray herbicides on weeds in the fields. Numerous methods [6-10] have been developed for weed classification but they lack classification accuracy and are not robust to varying field conditions. Hence, the superlative set of features and classification approach is yet to be discovered [1, 11].

The intelligent sprayer systems such as those equipped with visual sensors along with a mechanical sprayer, capture images from the field which are then processed for detecting the existence of weeds [12-15]. The detected weeds are then classified into monocots and dicots and lastly suitable signals are sent to the sprayer system for applying herbicides to the detected weed patches. Visual features such as texture, color, and shape are typically extracted from the captured images. Texture based features have been extensively applied for weed classification [16]. Previous methods of weed classification utilized features such as leaf shape and plant structure [6, 17]. Later on, some color and texture based methods [6] were also proposed. Nevertheless, majority of the techniques fail to balance the efficiency and effectiveness of weed classification in terms of processing speed and accuracy. Therefore, the goal is to develop a fast technique which is suitable for real time weed classification, avoiding unnecessary computations, and providing accurate classification under varying field environments.

To achieve such a system, researchers from the last decade have presented various weed classification techniques [1, 18]. Ahmad et al. [19] utilized simple statistical features for weeds classification, achieving a low accuracy as the technique utilized too naïve features. To improve the accuracy, Siddiqi et al. [20] explored edge link detector, achieving an accuracy of 93% on a

small dataset. The authors in [8] utilized wavelets by extracting highest 200 coefficients and integrated them with the k-nearest neighbor classifier (K-NN) for classification, achieving an accuracy of 95%. This work was further improved by employing multi-level wavelet decomposition (MWD) based classification by extracting highest coefficients of the wavelet decomposed images, representing weeds. However, the method fails to work effectively under varying field conditions [21]. Faisal et al. [16] incorporated local binary patterns along with template matching and support vector machine (SVM) classifiers for weed classification. But, their technique demands for extra computation due to its feature invariance property. Their technique achieved 89% accuracy in case of template matching and 98% with radial basis function (RBF) kernel based SVM classifier. However, due to exploring expensive texture descriptors for making the method geometric transform invariance, the computational complexity increased, hence making it less suitable for real-time applications.

In an attempt to reduce complexity, image morphology features along with neural network classifier (ANN) have also been used for classification of weed images, taken from outdoor fields. Illumination invariant segmentation procedure helped in achieving an overall accuracy of 95.1% with ANN classifier [10]. Seven hue moments and six shape features were extracted from weed images to classify them into monocots and dicots with an accuracy of 85% [6]. The images used during the experiments contained very little weeds. It was not difficult to analyze the individual leaves. However, in many cases, high infestations of weed are found throughout the fields and analyzing individual leaves become impractical. Therefore, in high weed infestations these methods would fail to perform. A similar study was conducted in [9], employing seven hue moments for weed classification. This method also failed to cope with high weed densities. Giselsson et al. [22] utilized close contour shape features to distinguish between two classes of plant seedling. They achieved 97.5% accuracy with Legendre Polynomial feature set while classifying nighshade and cornflower. Siddiqi et.al [23] explored a new wavelets family for features extraction from weeds images which were later on minimized based on step-wise linear discriminant analysis, making them linearly separable. Classification was performed by SVM achieving an accuracy of 98.1% with symlet wavelet features. To increase the accuracy, a mixture of features were used by authors in [24], including co-occurrence matrix, Haralick features, shape analysis, and histogram features, classifying weeds from captured field images

while achieving an average accuracy of 97.6% for both types of weeds. However, these methods were evaluated on noise-free, blur-free images, and without taking into consideration the illumination changes being faced in the field. Furthermore, their method was computationally expensive, requiring 0.35 s for classifying an image.

The aforementioned methods exploited various features and classifiers for weed classification. However, none of the methods produce satisfactory results when coping with intense field conditions such as illumination variations, motion blur, and noise. Some of the methods achieved high accuracies but with huge computational complexity, making them unsuitable for real-time applications [16, 20]. Other techniques were computationally efficient but lack acceptable accuracy, decreasing its applicability in various areas of interest [8]. Furthermore, some of the existing methods fail to cope with various lighting conditions which further limit their accuracy [1]. Therefore, it is very important to exploit a method for weed classification, maintaining the balance between accuracy and efficiency.

In this paper, we propose a fusion based weed classification framework for overcoming the problems of existing methods in terms of classification accuracy, resiliency against various lighting conditions, and efficiency. The major contributions of this research work are as follows.

i. An efficient fusion based framework is proposed for effective weed classification, maintaining a balance between classification accuracy and efficiency, hence making it more suitable for real-time applications such as selective herbicide sprayer systems.
ii. The proposed framework utilizes boosted visual features, incorporating both shape and texture information and are extracted using an efficient method, preserving the discrimination between various weed species and crops, hence results in satisfactory performance.
iii. The proposed framework uses an adaptive segmentation algorithm prior to feature extraction, minimizing the various illumination, noise, and motion blurring problems, hence making it more suitable for weed classification.
iv. A hybrid classifier AdaBoost ensemble of Naïve Bayes [25, 26] was used for classification, increasing the accuracy of current state-of-the-art weed classification methods.

The rest of this paper is structured as follows. Section 2 explains the detail of the proposed weed classification system. Section 3 explores experimental results and discussion. Section 4 concludes the paper and suggests future research directions.

2. Materials and Methods

In this section, we describe the detail of the proposed weed classification system. The proposed system comprises of two main phases: an offline training phase and a real-time classification phase. During the training phase, the main objective is the construction of a robust classifier model, having the capability to efficiently distinguish between two weed species in the presence of noise, illumination variation, and motion blurring. This objective is achieved by incorporating three steps in the proposed system. Firstly, an adaptive segmentation algorithm is used to handle the undesirable effects of noise, motion blur, and illumination during image acquisition. Secondly, visual features are extracted, incorporating both texture and shape, hence effectively drawing the boundaries between the two weed species. Finally, the AdaBoost along with Naïve Bayes classifier is used to train the classifier, resulting in the required classifier. During the testing phase, the same features are extracted from captured images and the appropriate label is then assigned to it based on which the sprayer system applies the appropriate herbicide to weed patches. The major steps of the proposed system are depicted in Fig. 1.

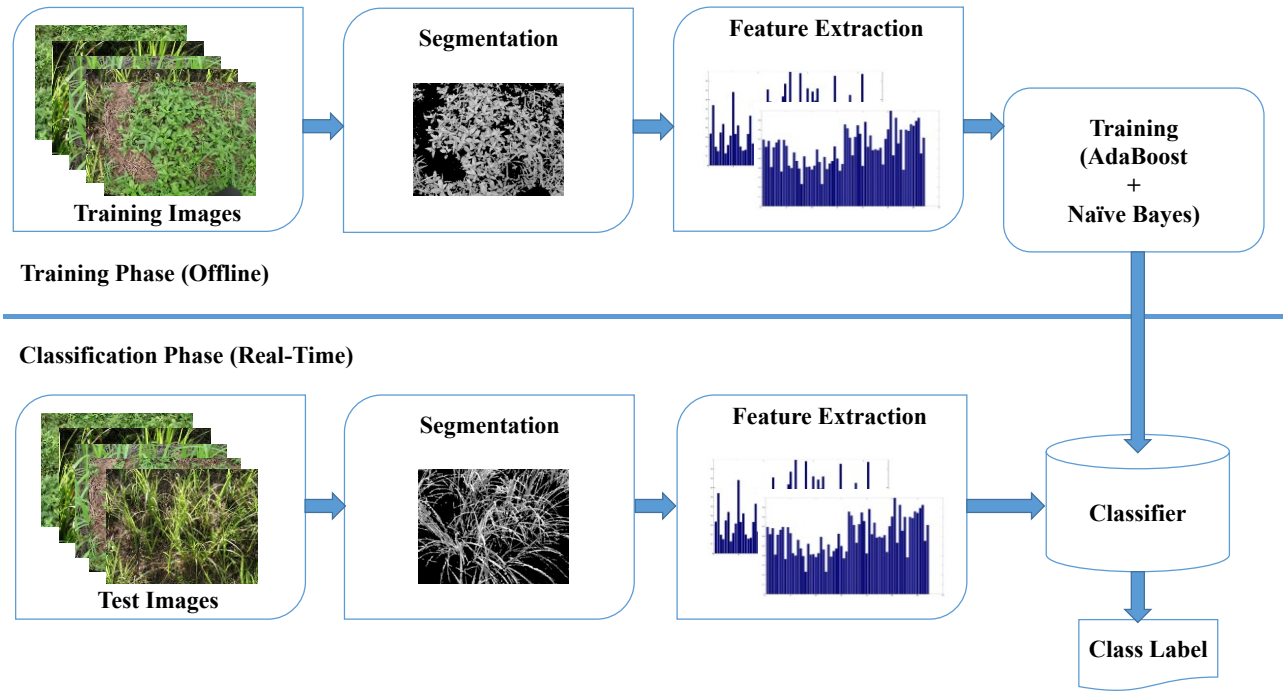

Fig. 1: The proposed weed classification system

2.1 Image Segmentation

Images captured from outdoor fields vary greatly in the illumination levels due to the varying lighting and weather conditions causing illumination variations, and shadows which affects the segmentation process. Several interesting studies have been carried out to deal with illumination variations [6] and vegetation segmentation in the presence of shadows [27]. In this paper, we attempt to devise an overall computationally efficient framework which can effectively deal with such circumstances. All the phases of the proposed framework has been designed in such a way that the subsequent module can effectively deal with any imperfections in the previous stage. For instance, the feature extraction process can tolerate with slight noise and motion blur which may cause slightly improper segmentation. Low quality sensors often introduce noise and motion blur during the image acquisition process. In order to achieve efficient segmentation, care must be taken to cope with these challenges. In addition to these issues, real-time systems need fast segmentation algorithms. Keeping in view all these constraints, a computationally efficient and adaptive segmentation procedure has been devised which dynamically computes threshold values for each image to segment the green components from the rest of the image. The purpose of

segmentation process is to eliminate background objects like ground and noise which may cause mis-classifications, prior to feature extraction. For an input image, $I \in R^{M \times N}$, a background elimination function is given in equation 1 as follows.

$$S = \begin{cases} 0.299 \times I_{\mathcal{R}} + 0.587 \times I_{\mathcal{G}} + 0.114 \times I_{\mathcal{B}}, & I_{\mathcal{G}} > I_{\mathcal{R}} \,\&\, I_{\mathcal{G}} > I_{\mathcal{B}} \,\&\, I_{\mathcal{G}} > \mathcal{T}_0 \\ 0, & \text{Otherwise} \end{cases} \quad (1)$$

Herein, I_R, I_G, and I_B represent red, green, and blue planes of the input image I, respectively. S shows the resultant output image produced by this phase. It encompasses either zeros indicating background pixels or grayscale values for the detected weeds, calculated based on standard color-to-gray conversion formula. For selection of optimal threshold value T_0 for each image in order to minimize the effect of illumination caused by environmental conditions, several experiments were conducted. It was found that the optimal value can be computed for each image dynamically using the mean intensity value of the image being observed as follows.

$$\mathcal{T}_0 = \alpha \frac{1}{\mathcal{MN}} \sum_x \sum_y I(x, y) \quad (2)$$

Where M and N are the dimensions of image (i.e. number of rows and columns), and α is an intensity gain factor used to control the threshold in different field and noise conditions. Applying simple noise reduction filters like mean and median filters help in keeping sustainable performance in case of noisy images. As a post- thresholding step, trivial objects may be removed from the segmented images using morphological opening with a small 3x3 disk shaped structuring element.

Minimizing the effects of the various image degradations is essential because incorrect segmentation leads to low performance [28, 29]. In addition to this, real-time systems require computationally in-expensive procedures. Therefore, segmentation algorithms consisting of simple steps with sufficient accuracy are most desirable. Initial work conducted in this regard either ignored illumination variation [8, 23, 30] or used computationally expensive procedures for segmentation [16, 31], which affects the overall framework adversely

2.2 Features Extraction

By observing both types of weeds from the captured images, it can be easily noticed that both species have the same color but different texture and leaf shapes. Therefore, both of these characteristics need to be quantified in a manner that will support the classification phase later in the process. Extraction of the texture and shape features is described in the following sub-sections.

A. Extraction of Edge Orientation Features

From the spatial layout of a variety of weeds including Southern Sandbur, Large Crabgrass, Curly Dock, Dallis grass, Nutsedge, Ground Ivy, and Spotted Spurge, etc., it was observed that both grass and broad leaf weeds have different edge distributions across the entire image especially during the stage when their leaves have somewhat grown in shape. Since, the edge orientation features can be effectively computed based on the leaves, the proposed method can be applied well before the flowering stage. This observation lead us to believe that capturing this characteristic will help in discriminative representation of the weeds. For this purpose, the edge orientation histogram (EOH) [32] feature was extracted from the images with slight modifications. Instead of blindly selecting the default 4 x 4 grid setup for computation of the EOH, we decided to experiment with different settings. Experiments were conducted to determine optimal number of grids for a certain height at which the images were captured in the field. Further details of the experiment are provided in section 3. The EOH feature represents texture by accumulating the number of edges having different orientations in the sub-images into a histogram. Edges of different orientations are detected using the Sobel filters [33] specified in Fig. 2. These filters detect horizontal, vertical, and diagonal (45 and 135) edges. The prominent edges are preserved, whereas the remaining of them are removed based on a simple threshold function, where the threshold value was chosen in a way to improve discriminative capability of the feature vector being computed. It is achieved by eliminating trivial edges from images of both weed types, because their presence affected the overall recognition performance. In this case, a fixed threshold value of 85 was chosen. Each bin in the EOH histogram correspond to the number of edges of a particular orientation in a particular sub-image. In this case, 4×4 sub-images resulted into $4 \times 4 \times 4 = 64$ bin histogram per image as a texture feature.

1	2	1
0	0	0
-1	-2	-1

(a)

-1	0	1
-2	0	2
-1	0	1

(b)

-2	-1	0
-1	0	1
0	1	2

(c)

0	1	2
-1	0	1
-2	-1	0

(d)

Fig. 2: Four filters for detection of (a) horizontal (b) vertical (c) diagonal at 45 and (d) diagonal at 135 degrees edges.

Broad weed leaves are circular in nature forming clusters of leaves across the fields. They produce almost equal number of edge pixels along all orientations. In contrast to this, grass weed leaves are longer producing comparatively longer edges at certain orientations. The EOH effectively captures these characteristics forming different histograms for the two weed species. The EOH histogram is computed by concatenating all the local orientation histograms as follows.

$$\mathcal{EOH} = \bigcup_{i=1}^{b} \mathcal{Bin}_i \tag{3}$$

Where EOH is the edge orientation histogram with b bins, each of which is calculated using equation 4 as follows.

$$\mathcal{Bin}_j = \sum \{ j \mid j \in S \wedge j \in \mathcal{E}_o \} \tag{4}$$

Where $S \in \{S_1, S_2, ...S_n\}$ and $E_o \in \{0, 45, 90, 135\}$, Bin_j is the j^{th} bin value which represents the number of edge pixels belonging to a particular edge-type and a particular sub-image S. It was also observed that textural features alone cannot adequately model both weeds. Therefore, local shape features are also used along texture to allow accurate classification. For allowing the fusion of the two features, the EOH is normalized to the range [0, 1] using the equation 5 as follows.

$$\mathcal{EOH}_n = \frac{\mathcal{EOH}}{\max(\mathcal{EOH})} \tag{5}$$

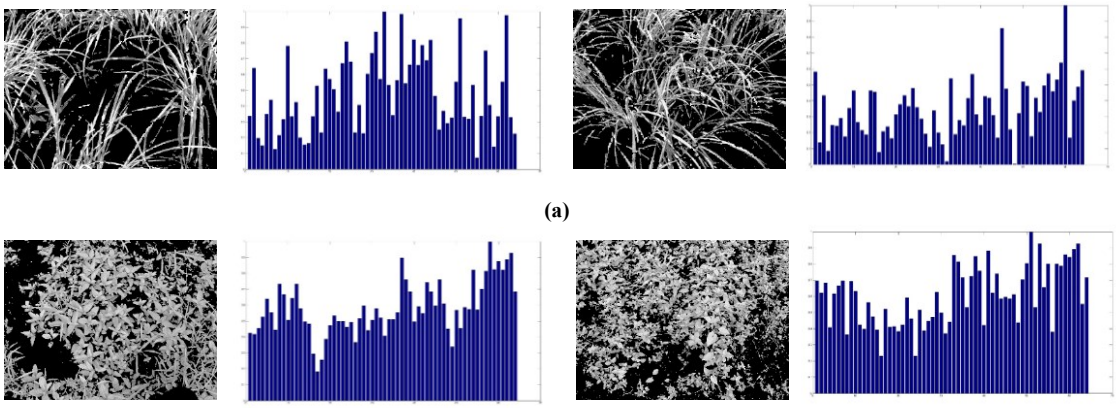

(a)

(b)

Fig. 3: Segmentation results. (a) Segmented grass weed images and their EOH (b) Broadleaf weed segmented images with their EOH.

In Fig. 3(a), it can be noticed from the segmented images containing grass weeds, that there exists more edges at certain orientations due to the lengthy nature of the leaves. This characteristic of the grass weeds is reflected in the EOH having higher values at certain orientations and lower values at other orientations. In contrast to this, the EOH of corresponding broad weed images in Fig. 3(b) shows relatively lower variation in the number of edges at different orientations. This uniformity in edge distributions at all orientations signify the roundness of broad leaves. Hence, the EOH descriptor effectively captures distinctive features of the two weed species.

In order to exhibit the discriminative characteristics of the EOH descriptor for the two weed species, Fig. 4 shows the mean feature vectors for both classes along with standard deviation of each feature. It can be seen that there exist significant variations in most of the features which eventually assist the classification stage in making accurate predictions.

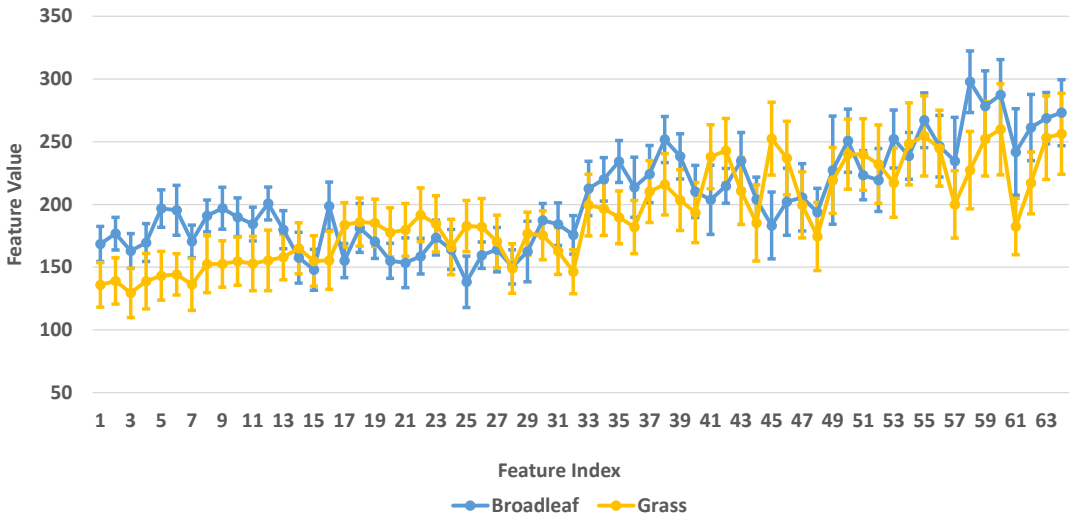

Fig. 4. Mean feature vectors (EOH) of both weed types with standard deviations

B. Shape Matrix Histogram (SMH)

In addition to texture, local shape features of the weeds are also captured using a grid based local feature extraction approach [34, 35]. Since the weed leaves in these images are mostly overlapped, it becomes difficult to isolate them and analyze their shapes individually. Global shape analysis also becomes ineffective due to the high degree of overlap in both weed types. Therefore, local shape features are extracted by dividing the entire image into d × d sub-images. The shape of leaves in each grid cell is analyzed. In order to capture the thickness/roundness or thinness of the leaves, local coverage feature is computed for all cells in the image. Broad leaves tend to produce more cells with higher coverage values than thinner leaves, allowing us to capture structure of the objects contained in the image. The layout of leaves in grid cells is illustrated in Fig. 5. It can be seen from close observation, that the area covered by broad leaf is large, hence, there exists larger number of grid cells that are almost fully covered by leaves. This characteristic is also used for discrimination between the two weed species.

(a) (b)

Fig. 5. Leaf structure inside grid cells. (a) A sample of broad leaves (b) A sample of thinner leaves.

The coverage feature for each cell is computed using equation 6 as follows.

$$\mathcal{R}_c = \frac{\mathcal{A}_s}{\mathcal{A}_c} \tag{6}$$

Herein, R_c represents coverage value of cell c, A_s shows the area of the leaf inside cell c, and A_c is the grid cell area. In broad weed image, there will be higher cell count with larger R_c compared to grass weed image. Similarly, there will be higher cell count with smaller R_c values in grass weed images. These R_c values obtained from the grid cells form a shape matrix $SM \in R^{d \times d}$. For reducing the feature dimension and capturing the essence of this matrix, a histogram is populated by quantizing the values in SM into 10 bins. The quantization strategy is depicted in equation 7 as given.

$$\mathcal{SMH}_i = \sum_i \left(\left\lceil \mathcal{R}_c^i \times 10 \right\rceil = i \right), \quad i = \{1,2,3,...10\} \tag{7}$$

The SMH feature for grass and broadleaf weed types is shown in Fig. 6. From the shape matrix (middle), it can be seen that the number of grid cells having higher R_c values in broad weed image is much higher than the others. Grid cells with higher R_c values are represented in red color, whereas lower R_c values are shown in blue color. The dark blue portion of the image

represents the background. Cells in light blue color indicate narrower structures (grass leaves), whereas cells in red color indicate bigger structures (broadleaf leaves). The SMH (right) clearly shows different histograms for both weed species. The SMH of grass weed shows relatively uniform distribution of quantized R_c values in the shape matrix. There is little difference in the distribution of higher R_c values and the rest. In contrast to this, the SMH of broad weed image shows a huge difference in the number of cells with R_c values > 0.9 and the rest. The SMH feature analyzes weed images locally and represents local structures in a compact way. It can be seen from both images that there exists sufficient discrimination in the SMH of both species, which allows their classification with higher accuracy.

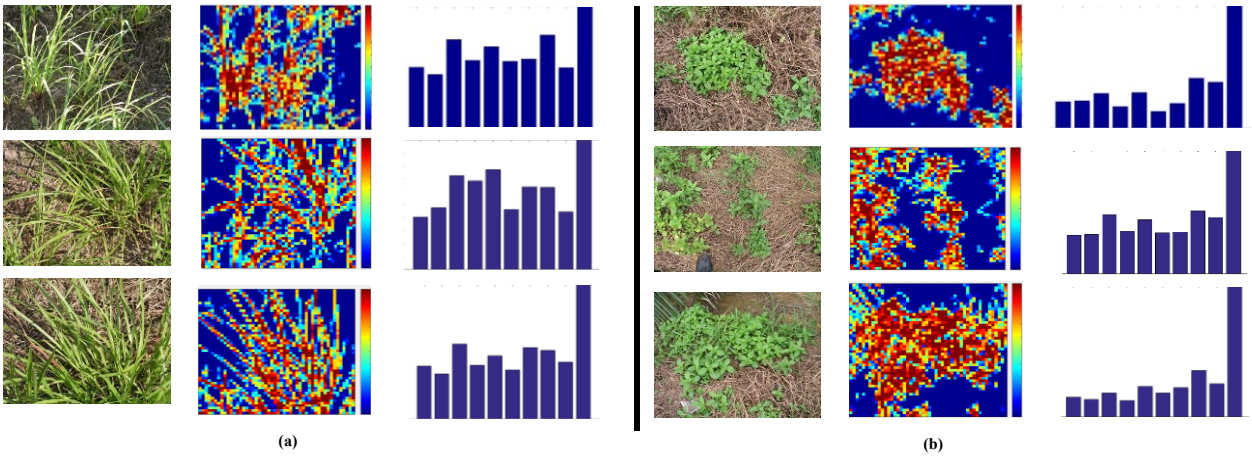

Fig. 6. Weeds and their corresponding shape matrix histograms. (a) grass weed image, its shape matrix, and shape matrix histogram (b). Broad weed image, its shape matrix, and shape matrix histogram

In addition to this, the shape matrix can also be used to localize the two weed types in a single image. Broad and grass weed leaves can be easily detected by analyzing their SMs. Grid regions with dense clusters of higher R_c values represent broad weeds, whereas grid cells with lower R_c values indicate grass weeds. Mean feature vectors of both weed classes are illustrated in Fig 7 to provide an insight on the discriminative ability of feature vectors. Finally, the 64-bin EOH and 10-bin SMH features are combined to form a single 74 dimensional feature vector. The normalized values of both these features are concatenated to form a signature for representing weeds as follows.

$$Sig = \bigcup(\mathcal{EOH}, \mathcal{SFH}) \tag{8}$$

Fig. 7 shows the comparison of SMH for both weed types. The mean feature vectors for broad leaf weed and grass clearly shows that there exist variations at almost all the feature values except feature 7. This class-wise discrimination provides a solid foundation upon which the classification stage can make confident and accurate predictions.

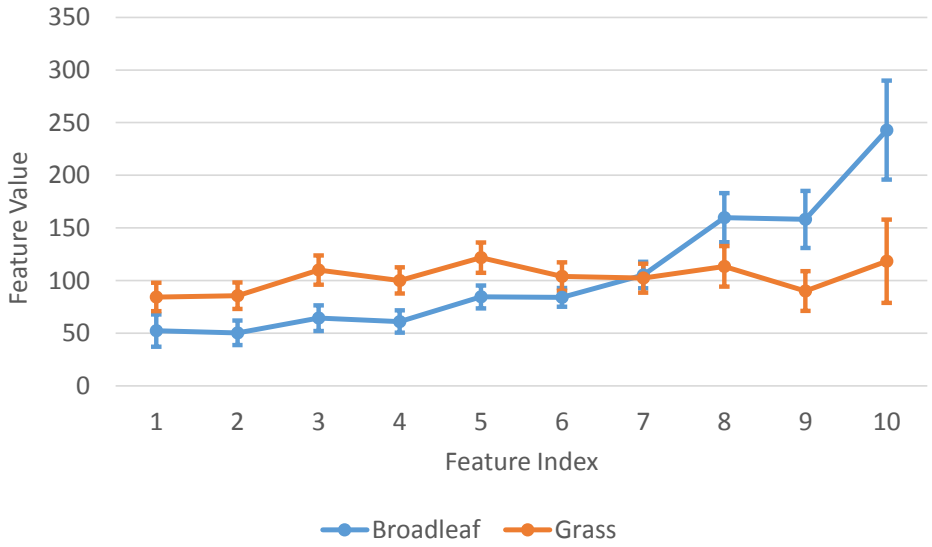

Fig. 7: Mean feature vectors (SMH) of both weed types with standard deviations

3. Experimental Results and Discussion

In this section, we illustrate the complete experimental setup for the proposed framework and evaluate its performance from different viewpoints. The proposed framework is implemented using MATLAB R2014a on a PC running Windows 7 professional with 8 GB RAM and 3.40 GHz Core i5 processor.

3.1 Dataset

We have used a dataset of 500 images (250 images of each weed type) for evaluation of the proposed framework. The images included in the dataset were acquired from outdoor fields under varying lighting and environmental conditions in resolution 320 x 240 from fields in the Khyber Pakhtunkhwa province, Pakistan. In order to comprehensively evaluate performance of the system in varying field conditions, images were captured during different times of the day and under different weather conditions. Furthermore, attempts were made to induce motion blur

during the image capturing process. To further test the robustness of our method, five different levels of noise was introduced in images by adding zero mean Gaussian noise having variance 0.01 to 0.05. This helped in building a much diverse dataset that will allow comprehensive evaluation of the proposed scheme. These synthesized images containing noise were added to both training and test sets. All the experiments were conducted using 10 folds cross validation where 90% of the data was used for training and the remaining 10% was used for testing in each fold.

Average classification accuracy was used to measure the performance of the proposed scheme. It is the ratio of correctly classified samples to the total number of samples in the dataset. Ideally, higher accuracies are desired under all circumstances. It shows the overall strength of the algorithm in performing the intended tasks.

$$Accuracy = \frac{Num_{CorrectlyClassified}}{TotalNum} \times 100 \tag{9}$$

Various experiments were conducted to test the performance of all the three modules in the proposed framework. The details of experiments and their results are provided in the subsequent sections.

3.2 Performance Evaluation of the Proposed Adaptive Segmentation Algorithm

Image segmentation is the first phase in the framework and undoubtedly the most important one because the performance of the subsequent modules heavily depend upon it. Accurate and robust segmentation procedure is the key to a successful machine vision system. In the present scenario, there were several challenges during the segmentation phase to cope with. Keeping in view these challenges, the performance of the proposed algorithm was evaluated using three different experiments. The details are given in the subsequent sections (section A, section B, and section C).

A. Effect of Illumination on Segmentation

For this test, images captured during variable environmental conditions were used. Illumination variation often produces undesirable segmentation results, affecting the features extraction process, which eventually lead to misclassifications. The adaptive nature of the proposed algorithm allowed it to handle illumination variations quite effectively. Some of the images along with the output of segmentation phase are provided in Fig. 8. The adaptive selection of the threshold value enables it to cope with varying lighting conditions in the fields, thereby producing similar output despite illumination variation. For low illumination, the classification performance dropped 1.5% and for higher illumination it dropped just under 1%.

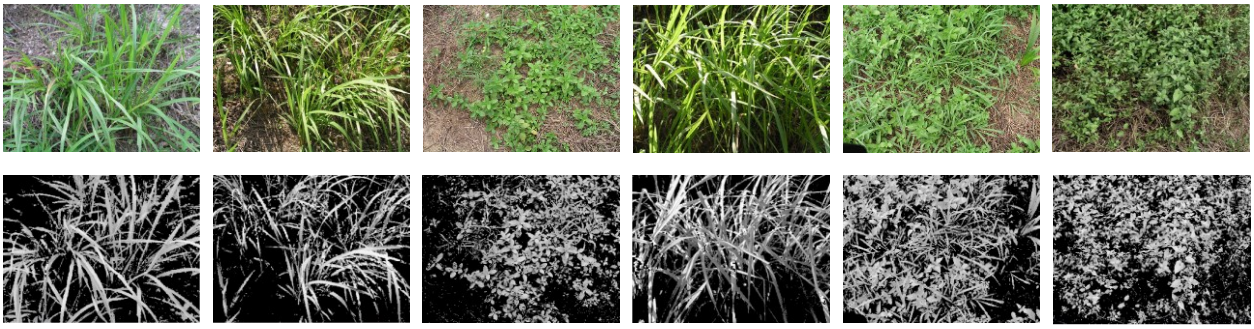

Fig. 8. Results of the proposed adaptive segmentation method under variable illumination. (a) Six images with varying illumination. (b) Corresponding segmented images produced by the proposed adaptive segmentation scheme

B. Effect of Motion Blur on Segmentation

Image capturing during motion produces blurriness in images which affects performance of the segmentation algorithm and overall classification, thereby making it necessary to investigate the effect of image blur. Hence, experiments were designed to evaluate performance of the proposed framework on blur images. Images were captured by modifying the speed of the camera to induce varying amounts of blur in them, so that its effect on performance could be evaluated. The segmentation algorithm, effectiveness and invariance of the extracted features, and the classifier, all contribute towards accuracy in such circumstances. Fig. 9 shows some visual results of the segmented blur images. It can be seen that with the varying degree of blur, the segmentation algorithm successfully removes the background. This is also evident from the classification results in Table 1, that there is only slight drop in performance when the degree of blur gets very high. With low blur, the performance drops by about 1%, whereas with high blur,

406 a drop of 7.5% was noticed. Since, the field camera motion is slow, chances of high blur are low.
407 Hence, performance hit with blurriness in real circumstances will be minimal.

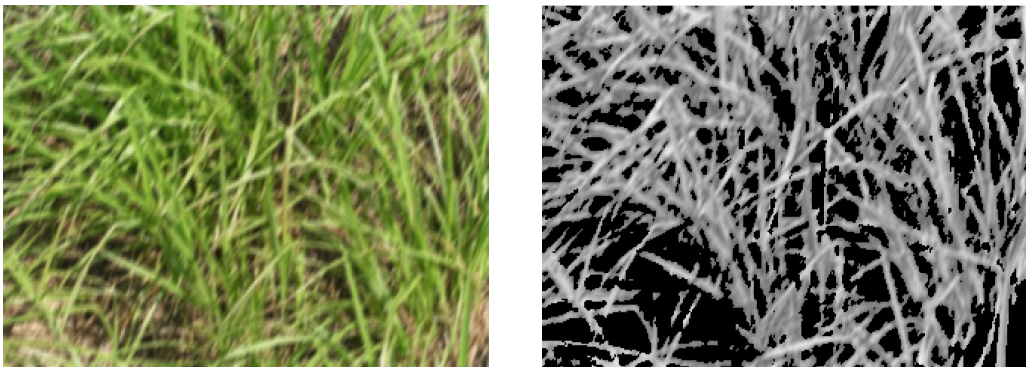

(a)

(b)

408

409 Fig. 9: Results of the proposed adaptive segmentation algorithm under motion blurring. (a)
410 Segmentation of grass weed blur image. (b) Segmentation of broadleaf weed blur image.

411

412 Table 1: Effect of image blur on performance using the proposed framework

Motion Blur Strength	Classification Performance (%)
Low	97.42
Medium	96.50
High	91.16

413

414 *C. Effect of Noise on Performance*

415 Varying field conditions, low illumination, and low quality imaging sensors introduce
416 noise in images. Noise causes significant performance drops in segmentation algorithms

[36]. In this case, gaussian noise of varying intensities was introduced in images prior to image segmentation to evaluate performance of proposed scheme. The classification performance without noise and with varying noise levels is given in Table 2. It was observed that noise causes a drop of 6-10% in accuracy when no removal attempt is made prior to image segmentation. However, this drop in accuracy was reduced to 2-5% when the noisy image was fitlered with a small mean filter. In the absence of noise, application of mean filter does affect performance slightly due to the blurring introduced. In Fig. 10, it can be seen that the noise has caused imperfect segmentation. However, these imperfections don't cause much trouble in the features extraction process due to the very nature of the feature being used. The presence of noise will affect the amount of edges produced by the edge detection filters, but most of the trivial edges caused by low intensity noise will be removed during the thresholding process. Furthermore, during the SMH feature extraction, the tiny dots in the background and the small holes in the foregrouond caused by noisy segmentations will not affect the feature dramatically. The classifier will still be able to classify them correctly, as is evident from the results in Table 2.

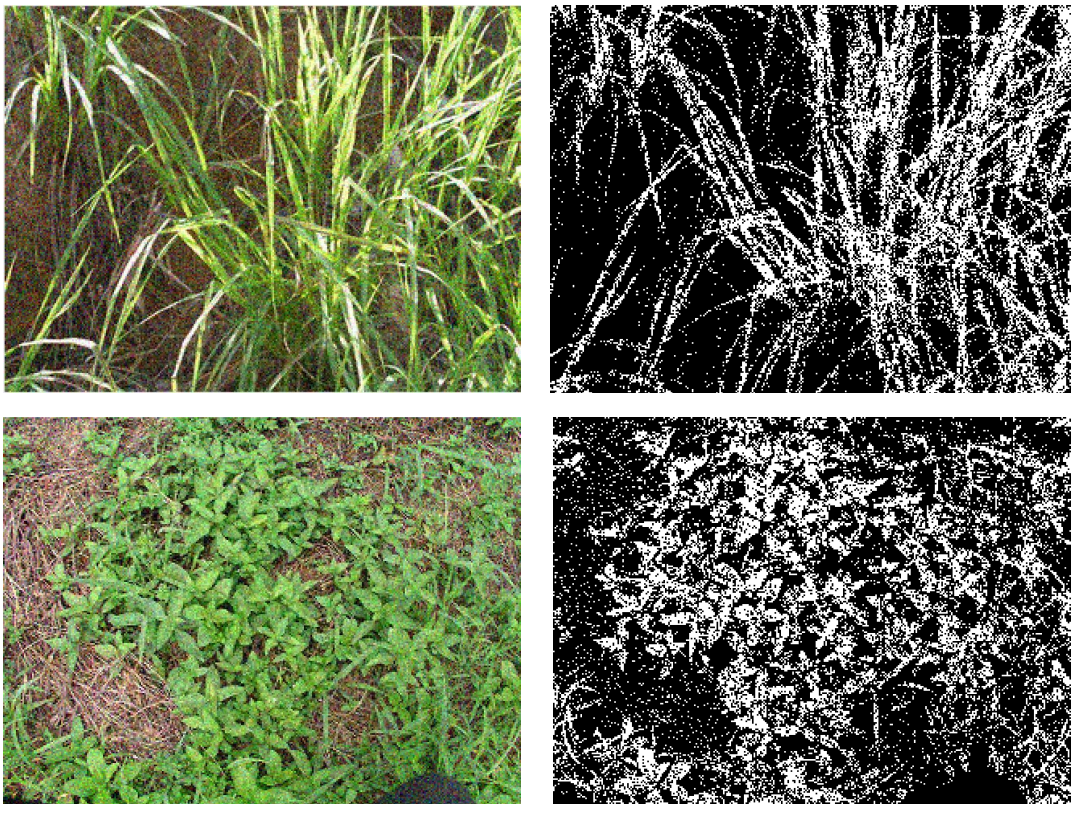

Fig. 10. Effect of noise on image segmentation (no filtering)

Table 2: Effect of noise on performance using the proposed framework

		Performance	
Noise Levels	Sigma (variance)	Without mean filtering (%)	With mean filtering (%)
No noise	-	98.40	98.29
1	0.01	91.32	96.23
2	0.02	90.95	95.1
3	0.03	89.42	94.56
4	0.04	88.00	93.42
5	0.05	87.61	92.85

3.3 Performance of Extracted Features

Optimal parameter selection is the key to optimal performance. Several experiments were carried out for determining the optimal set of parameter values for the proposed features extraction scheme. The shape features largely depend upon the grid cell size for local leaf structure estimation and the typical leaf sizes. Since, the leaf size depends upon the height of camera, it is important to derive a relation between camera heights and cell sizes. In order to allow sufficient discrimination between the two weed species, several grid sizes were investigated with images captured at varying heights. A performance drop was observed when cell size was set too small or too large, mainly because it failed to represent the two leaf structures discriminatively. For an image captured at a height of 1, 2, and 3 meters above ground, accuracies with varying cell sizes are given in Fig. 11. Cell sizes are shown in percentage of image sizes and can be computed using (10 and 11). For the current dataset containing image resolution of 320 x 240, setting the cell size to 2% of the image for images captured from a height of 2 m yields the best results. However, images captured at other heights have different optimal cell sizes.

$$patch\_width = \left\lceil \frac{patch\_size}{100} \times image\_width \right\rceil \quad (10)$$

$$patch\_height = \left\lceil \frac{patch\_size}{100} \times image\_height \right\rceil \quad (11)$$

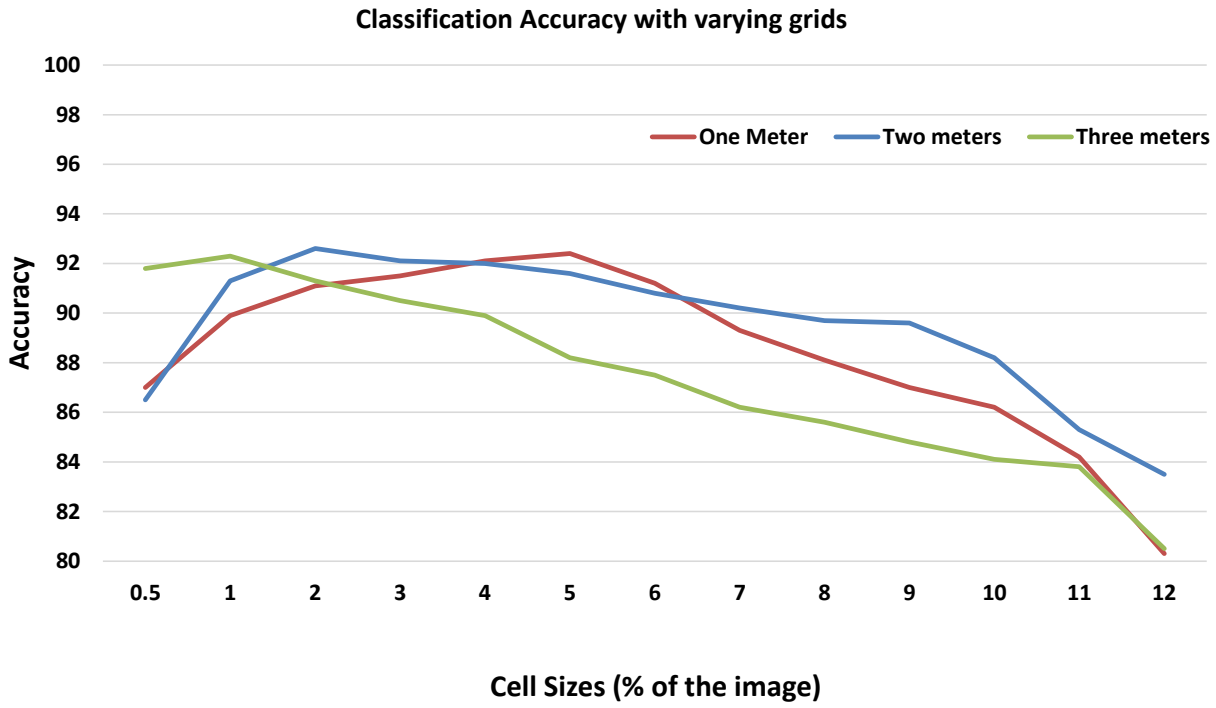

Fig. 11. Classification accuracies for varying cell sizes.

3.4 Classification Performance

Supervised learning has shown promising results in so many computer vision applications. Highly focused work is in progress for building new ways of building powerful models that achieve higher accuracies in solving complex problems. In addition to individual classifiers, ensembles of classifiers are also build to cope with highly complicated classification tasks. One such algorithm for generating ensemble of classifiers is AdaBoost [37]. It builds a combination of so-called weak classifiers through a strong learning algorithm i.e. AdaBoost. It has exhibited considerable improvements in comparison to individual classifiers.

The AdaBoost algorithm inputs labeled dataset (X, Y) = {(x1, y1),…(x_n, y_n)} where $x_n \in R^N$ is the N-dimensional feature vector used to classify the particular weed image, and $y_n \in \{-1, +1\}$ represents the classification labels for both weeds. It then calls the weak classifier or base learner iteratively. At every iteration, a weight is assigned and modified for each training sample x_i such that the weights of incorrectly classified samples gets enlarged forcing the weak learner to focus

on the difficult patterns in the training dataset. The base learner is only required to find a hypothesis $h_t : X \rightarrow Y$ for distribution D_t. The goodness of a hypothesis *h* is measured by its error ε at each iteration t as follows.

$$\varepsilon_t = \mathcal{P}[h_t(x_i) \neq y_i] = \sum_{i:h_t(x_i)\neq y_i} \mathcal{D}_t(i) \tag{12}$$

Upon calculation of h_t, AdaBoost selects a parameter $\alpha_t=(1/2)\ln(1-\varepsilon_t)/\varepsilon_t$ that is the weight of h_t signifying its importance. It is important to note that α_t gets large when ε_t gets smaller. The final hypothesis consists of a weighted majority vote of T weak hypotheses where α_t specifies the weights given to h_t. Thus, for each instance x_i, h_t outputs a prediction $h_t(x_i) \in R$ whose sign is the output label.

$$\hat{y} = f(x) = \operatorname{sgn}\left(\sum_{t=1}^{\mathcal{T}} \alpha_t h_t(x)\right) \tag{13}$$

In our case, several weak learners were tested with AdaBoost including Naïve Bayes [38], BayesNet [39], simple logistic regression [40], decision tree [41], and random tree [42]. Among these base classifiers, AdaBoost performed best with Naïve Bayes, reporting an overall accuracy of 98.16% for both weed types. Classification accuracies of 97.17%, 94.65%, and 98.16% were reported by AdaBoost + Naïve Bayes for EOH, SMH and EOH + SMH, respectively. The performance with the other configurations is provided in Fig. 12.

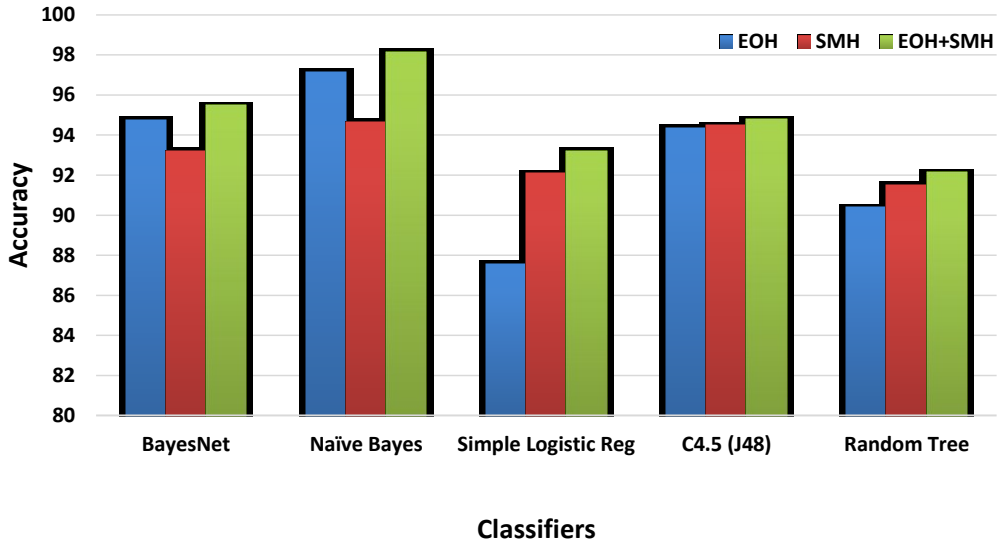

Fig. 12: Classification accuracies of the proposed framework with different classifiers.

3.5 Computation time analysis

In real-time computer vision systems, it is necessary to consider the execution time of data processing algorithms as it is the key to their applicability in real-time scenarios. In this section, we present the time taken by the various processing components of the proposed scheme. It can be seen from the Table 3, that the most computational expensive module is the EOH feature extraction because of the slightly heavy computations involved in computing local edge orientation histograms. SMH feature extraction module runs slightly faster than the EOH algorithm and requires on average 10 ms for each image. The prediction process requires about 4.5 ms and the segmentation process takes just under 2 ms. Overall, the whole scheme require 35.2 ms which make it suitable for real-time systems, since, it is capable of processing 28.4 frames per second.

Table 3: Execution time of various phases in the proposed method

Processing Module	**Execution Time (per image)**
Segmentation	1.7 ms
EOH Feature Extraction	19 ms
SMH Feature Extraction	10 ms
Classification	4.5 ms
Overall	**35.2 ms (28.4 fps)**

3.6 Comparison with other Methods

The proposed method was compared with seven other state-of-the-art methods, developed in the last 5 years. These methods use wavelet features, spatial analysis, local binary patterns, principal component analysis, and fusion based methods to discriminate grass from broad leaf weeds. The accuracies of all these methods with the dataset used, and their computation times are depicted in Table 4. All these methods performed exceptionally well with their datasets achieving above 90% classification accuracies. However, when we evaluated these methods on our expanded dataset which included images with varying illumination, motion blur, and slight noise, their performance dropped significantly. For instance, 22%, and 24% drops were noticed in the performance of combined strategy [9] and shape + fuzzy method [6] with our expanded dataset, because they evaluated their algorithms on very low weed infested areas. This is the highest performance drop among all the methods being compared. Similarly, significant drops in classification performance were noticed in the methods [8], [21], and [16], when these methods were evaluated using our dataset. The methods [24] and [23] used a combination of features to perform classification and hence were found to be relatively robust than the other methods. However, the method [24] carry a heavy computational cost due to the ensemble of two neural networks and combination of several computationally expensive features, which makes it unsuitable for real-time weed classification. In summary, it can be seen that the proposed method compares favorably, achieving 98.4% accuracy on the original dataset and 94.72% on the expanded datasets. Our method shows improved performance over the rest of the methods due to its robustness to illumination variation, motion blur, and noise. Table 4 lists comparison in terms of classification performance and computation time for the proposed method and other approaches. The computation times have been derived by running the algorithm on the same hardware platform.

Table 4: Classification accuracies with different classifiers.

Method	Classification Accuracy (original dataset)	Classification Accuracy (expanded dataset)	Computation Time
Combined Strategy [9]	92.63	71.45	135.0 ms
Shape + Fuzzy [6]	92.94	74.22	430.0 ms

Wavelet + KNN [8]	94.35	81.17	40.0 ms
MWD [21]	95.00	84.28	47.5 ms
Mixture Features [24]	97.66	91.66	350 ms
LBP + SVM [16]	98.00	85.14	45.4 ms
SWLDA + SVM [23]	98.10	92.87	40.5 ms
EOH + SMH + AdaBoost	**98.40**	**94.72**	**35.2 ms**

4. Conclusion and Future Research Directions

In this paper, the problem of weed classification was addressed by employing EOH and SMH features along with AdaBoost classifier for real-time herbicide sprayer systems. An adaptive and light-weight image segmentation algorithm was devised to eliminate background from the captured image. Special care was taken to account for changes in lighting conditions in the field, motion blur, and noise during the segmentation and feature extraction phase. It was observed that broad and grass weed images vary greatly in their shapes, causing different edge patterns and local shape structure across the entire image. In order to capture these discriminating characteristics, both texture and local shape features are extracted from the segmented weed images. A feature vector consisting of 74 values was constructed for each training image. AdaBoost algorithm was used to build an ensemble of Naïve Bayes classifier for weed classification. Experimental results reveal that the proposed scheme was able to classify weeds with high accuracies even in the presence of illumination variation, motion blur, and noise. An improvement of 4.7% was observed when compared with other state-of-the-art methods.

In our approach, the proposed shape features depend on the plant height as well as overlapping of leaves. Hence, it is necessary to optimally select the grid size corresponding to the height of the plants in the field. In future, we plan to use more powerful and robust hand-crafted features as well as feature engineering schemes to perform a fine-grained classification of many weed types and crops.

5. Acknowledgment

The authors are highly grateful to the anonymous reviewers and the associate editor for their prolific comments which significantly improved the quality of our work.

References

[1] D. C. Slaughter, D. K. Giles, and D. Downey, "Autonomous robotic weed control systems: A review," *Computers and Electronics in Agriculture,* vol. 61, pp. 63-78, 4// 2008.

[2] J. M. Green, "Current state of herbicides in herbicide-resistant crops," *Pest management science,* vol. 70, pp. 1351-1357, 2014.

[3] K. C. Swain, M. Nørremark, R. N. Jørgensen, H. S. Midtiby, and O. Green, "Weed identification using an automated active shape matching (AASM) technique," *Biosystems Engineering,* vol. 110, pp. 450-457, 12// 2011.

[4] M. S. Laursen, R. N. Jørgensen, H. S. Midtiby, K. Jensen, M. P. Christiansen, T. M. Giselsson*, et al.*, "Dicotyledon weed quantification algorithm for selective herbicide application in maize crops," *Sensors,* vol. 16, p. 1848, 2016.

[5] S. Chowdhury, B. Verma, and D. Stockwell, "A novel texture feature based multiple classifier technique for roadside vegetation classification," *Expert Systems with Applications,* vol. 42, pp. 5047-5055, 2015.

[6] P. J. Herrera, J. Dorado, and Á. Ribeiro, "A Novel Approach for Weed Type Classification Based on Shape Descriptors and a Fuzzy Decision-Making Method," *Sensors,* vol. 14, pp. 15304-15324, 2014.

[7] A. M. Naeem, I. Ahmad, M. Islam, and S. Nawaz, "Weed classification using angular cross sectional intensities for real-time selective herbicide applications," in *Computing: Theory and Applications, 2007. ICCTA'07. International Conference on*, 2007, pp. 731-736.

[8] I. Ahmad, M. H. Siddiqi, I. Fatima, S. Lee, and Y.-K. Lee, "Weed classification based on Haar wavelet transform via k-nearest neighbor (k-NN) for real-time automatic sprayer control system," in *Proceedings of the 5th International Conference on Ubiquitous Information Management and Communication*, 2011, p. 17.

[9] P. J. Herrera, J. Dorado, and Á. Ribeiro, "A New Combined Strategy for Discrimination between Types of Weed," in *ROBOT2013: First Iberian Robotics Conference*, 2014, pp. 469-480.

[10] H. Y. Jeon, L. F. Tian, and H. Zhu, "Robust crop and weed segmentation under uncontrolled outdoor illumination," *Sensors,* vol. 11, pp. 6270-6283, 2011.

[11] M. Loghavi and B. B. Mackvandi, "Development of a target oriented weed control system," *Computers and electronics in agriculture,* vol. 63, pp. 112-118, 2008.

[12] Y. Song, H. Sun, M. Li, and Q. Zhang, "Technology Application of Smart Spray in Agriculture: A Review," *Intelligent Automation & Soft Computing,* pp. 1-15, 2015.

[13] A. J. Ishak, A. Hussain, and M. M. Mustafa, "Weed image classification using Gabor wavelet and gradient field distribution," *Computers and Electronics in Agriculture,* vol. 66, pp. 53-61, 2009.

[14] J. I. Arribas, G. V. Sánchez-Ferrero, G. Ruiz-Ruiz, and J. Gómez-Gil, "Leaf classification in sunflower crops by computer vision and neural networks," *Computers and Electronics in Agriculture,* vol. 78, pp. 9-18, 2011.

[15] J. Ahmad, M. Sajjad, S. Rho, and S. W. Baik, "Multi-scale local structure patterns histogram for describing visual contents in social image retrieval systems," *Multimedia Tools and Applications,* vol. 75, pp. 12669–12692, 2016.

[16] F. Ahmed, H. Kabir, S. Bhuyan, H. Bari, and E. Hossain, "Automated Weed Classification with Local Pattern-Based Texture Descriptors," *International Arab Journal of Information Technology (IAJIT),* vol. 11, 2014.

[17] J. D. J. Herrera, and A. Ribeiro, "Application of the Dempster-Shafer theory to classify monocot and dicot weeds based on geometric shape descriptors," *Second International Conference on Robotics and associated High-technologies and Equipment for Agriculture and forestry,* pp. 149-156, 2014.

[18] E. Hamuda, M. Glavin, and E. Jones, "A survey of image processing techniques for plant extraction and segmentation in the field," *Computers and Electronics in Agriculture,* vol. 125, pp. 184-199, 2016.
[19] I. Ahmad, A. Muhamin Naeem, M. Islam, and A. Bin Abdullah, "Statistical Based Real-Time Selective Herbicide Weed Classifier," in *Multitopic Conference, 2007. INMIC 2007. IEEE International*, 2007, pp. 1-4.
[20] M. H. Siddiqi, I. Ahmad, and S. B. Sulaiman, "Edge link detector based weed classifier," in *Digital Image Processing, 2009 International Conference on*, 2009, pp. 255-259.
[21] M. Siddiqi, S. Sulaiman, I. Faye, and I. Ahmad, "A real time specific weed discrimination system using multi-level wavelet decomposition," *International Journal of Agriculture and Biology (Pakistan),* 2009.
[22] T. M. Giselsson, H. S. Midtiby, and R. N. Jørgensen, "Seedling discrimination with shape features derived from a distance transform," *Sensors,* vol. 13, pp. 5585-5602, 2013.
[23] M. H. SIDDIQI, S.-W. LEE, and A. M. KHAN, "Weed Image Classification using Wavelet Transform, Stepwise Linear Discriminant Analysis, and Support Vector Machines for an Automatic Spray Control System," *JOURNAL OF INFORMATION SCIENCE AND ENGINEERING,* vol. 30, pp. 1227-1244, 2014.
[24] W. Wong, A. Chekima, C. C. Wee, K. Brendon, and M. Marriappan, "Modular-based classification system for weed classification using mixture of features," *International Journal of Computational Vision and Robotics,* vol. 3, pp. 261-278, 2013.
[25] G. Camps-Valls and L. Bruzzone, "Kernel-based methods for hyperspectral image classification," *IEEE Transactions on Geoscience and Remote Sensing,* vol. 43, pp. 1351-1362, 2005.
[26] K. M. Ting and Z. Zheng, "A study of adaboost with naive bayesian classifiers: Weakness and improvement," *Computational Intelligence,* vol. 19, pp. 186-200, 2003.
[27] J. A. Marchant and C. M. Onyango, "Shadow-invariant classification for scenes illuminated by daylight," *Journal of the Optical Society of America A,* vol. 17, pp. 1952-1961, 2000/11/01 2000.
[28] A. Ribeiro, C. Fernández-Quintanilla, J. Barroso, M. García-Alegre, and J. Stafford, "Development of an image analysis system for estimation of weed pressure," in *Precision agriculture'05. Papers presented at the 5th European Conference on Precision Agriculture, Uppsala, Sweden.*, 2005, pp. 169-174.
[29] X. P. Burgos-Artizzu, A. Ribeiro, A. Tellaeche, G. Pajares, and C. Fernández-Quintanilla, "Analysis of natural images processing for the extraction of agricultural elements," *Image and Vision Computing,* vol. 28, pp. 138-149, 2010.
[30] I. Ahmed, Z. Ahmad, M. Islam, and A. Adnan, "A real-time specific weed recognition system by measuring weeds density through mask operation," in *Innovations and Advanced Techniques in Systems, Computing Sciences and Software Engineering*, ed: Springer, 2008, pp. 221-225.
[31] F. Ahmed, H. A. Al-Mamun, A. H. Bari, E. Hossain, and P. Kwan, "Classification of crops and weeds from digital images: A support vector machine approach," *Crop Protection,* vol. 40, pp. 98-104, 2012.
[32] M. Eom and Y. Choe, "Fast extraction of edge histogram in DCT domain based on MPEG7," in *Proceedings of world academy of science, engineering and technology*, 2005, pp. 209-212.
[33] N. Kanopoulos, N. Vasanthavada, and R. L. Baker, "Design of an image edge detection filter using the Sobel operator," *IEEE Journal of solid-state circuits,* vol. 23, pp. 358-367, 1988.
[34] J. Ahmad, M. Sajjad, I. Mehmood, S. Rho, and S. W. Baik, "Describing Colors, Textures and Shapes for Content Based Image Retrieval – A Survey," *Journal of Platform Technology,* vol. 2, pp. 34-48, Dec, 2014 2014.
[35] J. Ahmad, Z. Jan, and S. M. Khan, "A Fusion of Labeled-Grid Shape Descriptors with Weighted Ranking Algorithm for Shapes Recognition," *World Applied Sciences Journal,* vol. 31, 2014.
[36] J. Sauvola and M. Pietikäinen, "Adaptive document image binarization," *Pattern recognition,* vol. 33, pp. 225-236, 2000.

[37] R. E. Schapire, "The strength of weak learnability," *Machine learning,* vol. 5, pp. 197-227, 1990.
[38] A. McCallum and K. Nigam, "A comparison of event models for naive bayes text classification," in *AAAI-98 workshop on learning for text categorization*, 1998, pp. 41-48.
[39] N. Friedman, D. Geiger, and M. Goldszmidt, "Bayesian network classifiers," *Machine learning,* vol. 29, pp. 131-163, 1997.
[40] D. W. Hosmer Jr and S. Lemeshow, *Applied logistic regression*: John Wiley & Sons, 2004.
[41] D. M. Magerman, "Statistical decision-tree models for parsing," in *Proceedings of the 33rd annual meeting on Association for Computational Linguistics*, 1995, pp. 276-283.
[42] V. N. Vapnik and V. Vapnik, *Statistical learning theory* vol. 1: Wiley New York, 1998.